Symplectic and energy-conserving algorithms for solving magnetic field trajectories

Siu A. Chin
Department of Physics, Texas A&M University, College Station, Texas 77843, USA
(Received 29 May 2007; revised manuscript received 21 January 2008; published 3 June 2008)

The exponential splitting of the classical evolution operator yields symplectic integrators if the canonical Hamiltonian is separable. Similar splitting of the noncanonical evolution operator for a charged particle in a magnetic field produces exact energy-conserving algorithms. The latter algorithms evaluate the magnetic field directly with no need of a vector potential and are more stable with far less phase errors than symplectic integrators. For a combined electric and magnetic field, these algorithms from splitting the noncanonical evolution operator are neither fully symplectic nor exactly energy conserving, yet they behave exactly like symplectic algorithms in having qualitatively correct trajectories and bounded periodic energy errors. This work shows that exponential-splitting algorithms of any order for solving particle trajectories in a general electric and magnetic field can be systematically derived by use of the angular momentum operator of quantum mechanics. The use of operator analysis in this work fully comprehends the intertwining interaction between electric and magnetic forces and makes possible the derivation of highly nontrivial integrators.

DOI: 10.1103/PhysRevE.77.066401 PACS number(s): 52.65.Cc, 45.10.−b, 52.65.Yy

I. INTRODUCTION

The motion of a charged particle in a magnetic field $\mathbf{B}$ is governed by the Lorentz force law

$$m\frac{d\mathbf{v}}{dt}=q\mathbf{v}\times\mathbf{B}(\mathbf{r}). \tag{1}$$

In the usual formulation, this can be derived from a canonical but *nonseparable* Hamiltonian

$$H=\frac{1}{2m}[\mathbf{p}-q\mathbf{A}(\mathbf{r})]^2, \tag{2}$$

with $\nabla\times\mathbf{A}(\mathbf{r})=\mathbf{B}(\mathbf{r})$. Unfortunately, in terms of the canonical variables, the resulting equations of motion are of the "mixed variable" type, where the right-hand side (RHS) contains both variables $\mathbf{r}$ and $\mathbf{p}$,

$$\frac{d\mathbf{r}}{dt}=\frac{1}{m}[\mathbf{p}-q\mathbf{A}(\mathbf{r})], \tag{3}$$

$$\frac{d\mathbf{p}}{dt}=\frac{q}{m}[p_j-qA_j(\mathbf{r})]\nabla A_j(\mathbf{r}), \tag{4}$$

and cannot be used directly to develop symplectic integrators. To appreciate this point, recall the usual method [1–8] of constructing symplectic integrators for a nonmagnetic force $\mathbf{F}(\mathbf{r})=-\nabla V(\mathbf{r})$, which can be derived from a *separable* Hamiltonian with equations of motion:

$$\frac{d\mathbf{r}}{dt}=\frac{\mathbf{p}}{m}, \tag{5}$$

$$\frac{d\mathbf{p}}{dt}=\mathbf{F}(\mathbf{r}). \tag{6}$$

At its most basic level, the construction of symplectic integrators *does not* require the Hamiltonian formalism or Poisson brackets [9]; it only requires the equations of motion. Given any dynamical variable $W(\mathbf{r},\mathbf{p})$ (including $\mathbf{r}$ and $\mathbf{p}$ themselves), its evolution is given by

$$\frac{dW}{dt}=\frac{\partial W}{\partial\mathbf{r}}\cdot\frac{d\mathbf{r}}{dt}+\frac{\partial W}{\partial\mathbf{p}}\cdot\frac{d\mathbf{p}}{dt}$$

$$=\left(\frac{\mathbf{p}}{m}\cdot\frac{\partial}{\partial\mathbf{r}}+\mathbf{F}(\mathbf{r})\cdot\frac{\partial}{\partial\mathbf{p}}\right)W \tag{7}$$

$$=(T+V)W, \tag{8}$$

with the operator solution

$$W(t)=e^{t(T+V)}W(0). \tag{9}$$

Since the equations of motion (5) and (6) do not have mixed variables and the canonical variables $\mathbf{r}$ and $\mathbf{p}$ are classically independent, the Lie operators $e^{\varepsilon T}$ and $e^{\varepsilon V}$ are just *translation* operators,

$$e^{\varepsilon T}W(\mathbf{r},\mathbf{p})=W\left(\mathbf{r}+\varepsilon\frac{\mathbf{p}}{m},\mathbf{p}\right) \tag{10}$$

$$e^{\varepsilon V}W(\mathbf{r},\mathbf{p})=W(\mathbf{r},\mathbf{p}+\varepsilon\mathbf{F}(\mathbf{r})). \tag{11}$$

The general evolution operator can be approximated to any order via exponential splitting:

$$e^{\varepsilon(T+V)}\approx\prod_{i=1}^{N}e^{t_i\varepsilon T}e^{v_i\varepsilon V}, \tag{12}$$

with suitable coefficients $\{t_i,v_i\}$. The resulting sequence of alternating $\mathbf{r}$ and $\mathbf{p}$ translations then defines the corresponding algorithm, which happens to be symplectic [1–8]. In reviewing this derivation, we note two key steps: (a) We only need the equations of motion (5) and (6) to define the classical evolution operator (7). (b) The exponential splitting of the evolution operator via (12) produces well-defined algorithms if the component evolution operators $e^{\varepsilon T}$ and $e^{\varepsilon V}$ can be evaluated exactly. The fact that the resulting algorithms are symplectic is incidental to the derivation process. As long as the resulting algorithms have desirable numerical characteristics, whether we know or can name the property as being symplectic or not is irrelevant. Thus this method of exponen-

tial splitting can be applied to all equations of motion, as long as we know how to compute the component evolution operators exactly.

For equations of motion (3) and (4), because of the mixed variables, the corresponding component evolution operators cannot be evaluated in closed form and the naive construction fails. This explains the general lack of symplectic integrators for solving magnetic field problems. At first sight, since the fundamental Lorentz force law mixes both $\mathbf{v}$ and $\mathbf{r}$, the difficulty seemed intrinsic. Surprisingly, as will be shown in this work, the Lie operator corresponding to the Lorentz force law is just the *rotation* operator of quantum mechanics and can be evaluated in a closed form.

In trying to overcome this mixed variable problem in the canonical formulation, Wu, Forest, and Robin (WFR) [10] used gauge transformations to remove the potential $\mathbf{A}(\mathbf{r})$ at all intermediate steps of the algorithm. This procedure is workable, but rather cumbersome. The present work shows that exponential splitting, which yielded symplectic integrators when the equation of motion is unmixed, produces *exact energy-conserving* (EEC) algorithms when the equations of motion of a particle in a magnetic field are used. These two are exponential-splitting algorithms whose property we can name. For a combined electric and magnetic field, exponential splitting yields equally good algorithms that are neither fully symplectic nor exactly energy conserving, yet behaved identically as symplectic or EEC algorithms. At this time, we do not have a name to characterize the fundamental property of this class of algorithms.

This work will concentrate on solving the nonrelativistic magnetic field problem; its relativistic generalization will be considered elsewhere. We will begin by giving an alternative derivation of WFR's symplectic integrators in Sec. II so that we can compare them in Sec. IV with EEC algorithms derived in Sec. III. Exponential-splitting algorithms for integrating trajectories in a general electric and magnetic field will be derived in Sec. V and compared in Sec. VI. The present operator analysis is well suited for understanding the intertwining interaction between magnetic and nonmagnetic forces. Exact algorithms for solving constant fields are deferred to two appendixes.

II. SYMPLECTIC ALGORITHMS

In this section, we give an independent derivation of WFR's symplectic integrators [10] for solving magnetic field problems. This direct operator approach gives further insight into the form of these algorithms. The evolution operator corresponding to the equations of motion (3) and (4) is

$$\mathcal{T}=\exp\left[\frac{\varepsilon}{m}(p_j-a_j)\frac{\partial}{\partial r_j}+\frac{\varepsilon}{m}(p_j-a_j)(\nabla_i a_j)\frac{\partial}{\partial p_i}\right], \quad (13)$$

where in this section $a_i(\mathbf{r})=qA_i(\mathbf{r})$. Repeated indices are summed over. The sum over j corresponds to the full Hamiltonian (2). If j is fixed and not summed over, then the evolution operator $\mathcal{T}$ corresponds only to the j-direction Hamiltonian $(p_j-a_j)^2/2m$. (The index i is always summed over.) Because of the mixed variables, even if $\mathcal{T}$ were split, neither of its part could be exactly evaluated. Following WFR's idea, we seek to decompose $\mathcal{T}$ further in the form

$$\mathcal{T}'=\exp\left(f_i(\mathbf{r})\frac{\partial}{\partial p_i}\right)\exp\left(\varepsilon\frac{p_j}{m}\frac{\partial}{\partial r_j}\right)\exp\left(-f_i(\mathbf{r})\frac{\partial}{\partial p_i}\right), \quad (14)$$

where each exponential is a simple translation operator as in (10) and (11). Since

$$e^C\exp(K)e^{-C}=\exp(e^C K e^{-C}) \quad (15)$$

and

$$e^C K\, e^{-C}=K+[C,K]+\frac{1}{2}[C,[C,K]]+\frac{1}{3!}[C,[C,[C,K]]]+\cdots, \quad (16)$$

identifying $K=\varepsilon\frac{p_j}{m}\frac{\partial}{\partial r_j}$ and $C=f_i(\mathbf{r})\frac{\partial}{\partial p_i}$ gives

$$[C,K]=\frac{\varepsilon}{m}\left[f_j\frac{\partial}{\partial r_j}-p_j(\nabla_j f_i),\frac{\partial}{\partial p_i}\right],$$

$$\frac{1}{2}[C,[C,K]]=\frac{\varepsilon}{m}\left[-f_j(\nabla_j f_i)\frac{\partial}{\partial p_i}\right], \quad (17)$$

and all higher-order commutators vanish. Thus we have

$$\mathcal{T}'=\exp\left[\frac{\varepsilon}{m}(p_j+f_j)\frac{\partial}{\partial r_j}-\frac{\varepsilon}{m}(p_j+f_j)(\nabla_j f_i)\frac{\partial}{\partial p_i}\right]. \quad (18)$$

Note that the indices in $(\nabla_j f_i)$ are exchanged as compared to $(\nabla_i a_j)$ in (13). It might appear that $\mathcal{T}'$ will be equal to $\mathcal{T}$ if we set

$$f_j(\mathbf{r})=-a_j(\mathbf{r}). \quad (19)$$

This is not the case; because of the exchanged indices, even with (19), $\mathcal{T}'$ can only be equal to $\mathcal{T}$ if

$$\nabla_j a_i=\nabla_i a_j, \quad (20)$$

which means only for the trivial case of $\mathbf{B}=0$. However, if j is not summed over, then we only have a single term a_j. Satisfying the index requirement

$$\nabla_j f_i=-\nabla_i a_j \quad (21)$$

by demanding

$$f_i=-\int^{r_j}\nabla_i a_j(r_j')dr_j' \quad (22)$$

would simultaneously satisfy (19). Thus $\mathcal{T}$ can only be decomposed as $\mathcal{T}'$ in *each direction*. Denoting the j-direction operator in (13) as H_j, for a first-order algorithm, one can first factorize

$$e^{\varepsilon(H_x+H_y+H_z)}\approx e^{\varepsilon H_x}e^{\varepsilon H_y}e^{\varepsilon H_z} \quad (23)$$

and then replace $e^{\varepsilon H_j}$ in each direction via (14). Since each application of (14) requires two momentum updates, this algorithm doubles the number of momentum evaluations as compared to a first-order nonmagnetic symplectic algorithm. For a second-order algorithm, one can first factorize

$$e^{\varepsilon(H_1+H_2+H_3)} \approx e^{(1/2)\varepsilon H_x} e^{(1/2)\varepsilon H_y} e^{\varepsilon H_z} e^{(1/2)\varepsilon H_y} e^{(1/2)\varepsilon H_x} \quad (24)$$

(or any other permutation of H_x, H_y, H_z) and then make the replacement (14). This requires ten momentum and five coordinate updates. A nonmagnetic second-order algorithm only needs three momentum and six coordinate updates. Since updating the momentum requires a force or field evaluation, it is generally the more expensive operation. Thus this algorithm triples the computational effort of a second-order nonmagnetic algorithm. More generally, the factorization of three operators to higher order is more complex. In the original work of Wu, Forest, and Robin [10], the only fourth-order algorithm cited is the Forest-Ruth [1] integrator, which can be concatenated from three second-order algorithms. At even higher order, the number of momentum evaluations would proliferate even more unfavorably. In the next section, we will examine alternative algorithms for solving magnetic field problems.

III. EXACT ENERGY-CONSERVING ALGORITHMS

Since the cross product is defined by the right-hand rule, the description of a *negatively* charged particle in a magnetic field is more natural without an annoying negative sign. Throughout this paper we will therefore take

$$q = -e, \quad (25)$$

so that (1) reads

$$\frac{d\mathbf{v}}{dt} = \omega \hat{\mathbf{B}} \times \mathbf{v}, \quad (26)$$

where $\hat{\mathbf{B}}$ is the unit vector pointing in the direction of the magnetic field and

$$\omega(\mathbf{r}) = \frac{eB(\mathbf{r})}{m} \quad (27)$$

is the local cyclotron angular frequency. The dynamics is complete with the position equation

$$\frac{d\mathbf{r}}{dt} = \mathbf{v}. \quad (28)$$

In the noncanonical Hamiltonian approach (see below), $\mathbf{r}$ and $\mathbf{v}$ are to be regarded as independent variables. Equation (28) is the dynamical equation for determining $\mathbf{r}$ given $\mathbf{v}$.

For any dynamical variable $W(\mathbf{r},\mathbf{v})$, its evolution is given by

$$\frac{dW}{dt} = \frac{\partial W}{\partial \mathbf{r}} \cdot \frac{d\mathbf{r}}{dt} + \frac{\partial W}{\partial \mathbf{v}} \cdot \frac{d\mathbf{v}}{dt} = \left[\mathbf{v} \cdot \frac{\partial}{\partial \mathbf{r}} + \omega(\hat{\mathbf{B}} \times \mathbf{v}) \cdot \frac{\partial}{\partial \mathbf{v}} \right] W, \quad (29)$$

with the operator solution

$$W(t) = e^{t(T+V)} W(0), \quad (30)$$

where we have now defined

$$T = \mathbf{v} \cdot \frac{\partial}{\partial \mathbf{r}} \quad \text{and} \quad V = \omega(\hat{\mathbf{B}} \times \mathbf{v}) \cdot \frac{\partial}{\partial \mathbf{v}}. \quad (31)$$

Thus the simultaneous solution of (26) and (28) corresponds to the evolution operator $e^{t(T+V)}$. In particular, for $\varepsilon = \Delta t$, we have

$$\begin{pmatrix} \mathbf{r}(\varepsilon) \\ \mathbf{v}(\varepsilon) \end{pmatrix} = e^{\varepsilon(T+V)} \begin{pmatrix} \mathbf{r} \\ \mathbf{v} \end{pmatrix}. \quad (32)$$

If $\mathbf{B}(\mathbf{r})$ is spatially dependent, the general solution of (32) in not known. However, its component parts can be easily computed. For example,

$$e^{\varepsilon T} \begin{pmatrix} \mathbf{r} \\ \mathbf{v} \end{pmatrix} = \begin{pmatrix} \mathbf{r} + \varepsilon \mathbf{v} \\ \mathbf{v} \end{pmatrix}, \quad (33)$$

$$e^{\varepsilon V} \begin{pmatrix} \mathbf{r} \\ \mathbf{v} \end{pmatrix} = \begin{pmatrix} \mathbf{r} \\ \mathbf{v}_B(\mathbf{r},\mathbf{v},\varepsilon) \end{pmatrix}, \quad (34)$$

where we have defined

$$\mathbf{v}_B(\mathbf{r},\mathbf{v},\varepsilon) \equiv \mathbf{v} + \sin\theta(\hat{\mathbf{B}} \times \mathbf{v}) + (1 - \cos\theta)\hat{\mathbf{B}} \times (\hat{\mathbf{B}} \times \mathbf{v}), \quad (35)$$

with

$$\theta = \omega(\mathbf{r})\varepsilon. \quad (36)$$

Equation (35) follows because

$$\begin{aligned} \mathbf{v}_B(\mathbf{r},\mathbf{v},\varepsilon) &= e^{\varepsilon V}\mathbf{v} \\ &= \left(1 + \varepsilon V + \frac{1}{2}\varepsilon^2 V^2 + \frac{1}{3!}\varepsilon^3 V^3 + \cdots\right)\mathbf{v} \\ &= \mathbf{v} + \theta(\hat{\mathbf{B}} \times \mathbf{v}) + \frac{\theta^2}{2!}\hat{\mathbf{B}} \times (\hat{\mathbf{B}} \times \mathbf{v}) \\ &\quad + \frac{\theta^3}{3!}\hat{\mathbf{B}} \times [\hat{\mathbf{B}} \times (\hat{\mathbf{B}} \times \mathbf{v})] + \cdots \end{aligned} \quad (37)$$

and

$$\hat{\mathbf{B}} \times [\hat{\mathbf{B}} \times (\hat{\mathbf{B}} \times \mathbf{v})] = -\hat{\mathbf{B}} \times \mathbf{v}. \quad (38)$$

If we define

$$\mathbf{v} = \mathbf{v}_\parallel + \mathbf{v}_\perp, \quad (39)$$

where $\mathbf{v}_\parallel$ and $\mathbf{v}_\perp$ are components of $\mathbf{v}$ parallel and perpendicular to $\hat{\mathbf{B}}$, then (35) takes the transparent form

$$\mathbf{v}_B(\mathbf{r},\mathbf{v},\varepsilon) \equiv \mathbf{v}_\parallel + \cos\theta\mathbf{v}_\perp + \sin\theta(\hat{\mathbf{B}} \times \mathbf{v}_\perp), \quad (40)$$

where only $\mathbf{v}_\perp$ is rotated by $\mathbf{B}$. For a constant $\mathbf{B}$, $\mathbf{v}_B(\mathbf{v},\varepsilon)$ has no spatial dependence. Note that V can also be written as

$$V = \omega\hat{\mathbf{B}} \cdot \left(\mathbf{v} \times \frac{\partial}{\partial \mathbf{v}}\right) = i\omega\hat{\mathbf{B}} \cdot \mathbf{J},$$

where $\mathbf{J} = -i\mathbf{v} \times \partial/\partial\mathbf{v}$ is the "angular momentum" operator in v space and

$$\exp(\varepsilon V) = \exp(i\theta \hat{\mathbf{B}} \cdot \mathbf{J})$$

is the rotation operator which rotates the initial vector $\mathbf{v}$ about the axis $\hat{\mathbf{B}}$ by an angle θ. The final vector is then $\mathbf{v}_B(\mathbf{r},\mathbf{v},\varepsilon)$. See any graduate text on quantum mechanics—e.g., Ref. [11].

At the same time, $e^{\varepsilon V}$ is also a classical Lie operator which acts on any dynamical variable in the phase space $(\mathbf{r},\mathbf{v})$—in particular,

$$e^{\varepsilon V} v^2 = v^2. \tag{41}$$

This, together with

$$e^{\varepsilon T} v^2 = v^2, \tag{42}$$

implies that

$$\left(\prod_{i=1}^{N} e^{t_i \varepsilon T} e^{v_i \varepsilon V} \right) v^2 = v^2, \tag{43}$$

which means that all splitting algorithms of the above form are ECC. Note that this proof does not require knowing how $\mathbf{v}$ is rotated by $e^{\varepsilon V}$. Thus the use of $e^{\varepsilon V}$ is far more than just integrating (26) with $\mathbf{B}$ fixed.

The simplest second-order splitting

$$\mathcal{T}_{2a} = e^{(1/2)\varepsilon V} e^{\varepsilon T} e^{(1/2)\varepsilon V} = e^{\varepsilon W}, \tag{44}$$

with

$$W = T + V - \frac{1}{24}\varepsilon^2 [V,[V,T]] + \frac{1}{12}\varepsilon^2 [T,[T,V]] + \cdots, \tag{45}$$

yields the following algorithm 2a:

$$\mathbf{v}_1 = \mathbf{v}_B\left(\mathbf{r},\mathbf{v},\frac{1}{2}\varepsilon\right),$$

$$\mathbf{r}_1 = \mathbf{r} + \varepsilon \mathbf{v}_1, \tag{46}$$

$$\mathbf{v}_2 = \mathbf{v}_B\left(\mathbf{r}_1,\mathbf{v}_1,\frac{1}{2}\varepsilon\right), \tag{47}$$

where $\mathbf{r}$ and $\mathbf{v}$ are the initial values and the last numbered variables in (46) and (47) are the updated results. This is the magnetic field generalization of the velocity-Verlet algorithm. Similarly, the factorization

$$\mathcal{T}_{2b} = e^{(1/2)\varepsilon T} e^{\varepsilon V} e^{(1/2)\varepsilon T} \tag{48}$$

yields the following second-order algorithm 2b:

$$\mathbf{r}_1 = \mathbf{r} + \frac{1}{2}\varepsilon \mathbf{v},$$

$$\mathbf{v}_1 = \mathbf{v}_B(\mathbf{r}_1,\mathbf{v},\varepsilon), \tag{49}$$

$$\mathbf{r}_2 = \mathbf{r}_1 + \frac{1}{2}\varepsilon \mathbf{v}_1. \tag{50}$$

For higher-order algorithms, all conventional composition schemes [4–7] can now be used to solve (26) and (28) in an arbitrary magnetic field $\mathbf{B}(\mathbf{r})$.

For a uniform magnetic field, by analyzing the higher-order commutators in (45), this operator formalism can yield algorithms that are exact. See Appendix A for details.

All splitting algorithms can be generalized to solve the case of a time-dependent magnetic field by evaluating the magnetic field at an incremental time equal to the sum of time steps of all the preceding T operators. This is Suzuki's rule [12,13]. For algorithm 2a, if the time at the start of the algorithm is t, then evaluate the magnetic field initially at t and then at $t+\varepsilon$. For algorithm 2b, evaluate the magnetic field at $t+\varepsilon/2$. All such algorithms remain exactly energy conserving. For more discussions and examples of solving classical time-dependent force problems, see [14,15].

Finally, these EEC algorithms, in accordance with the Ge-Marsden theorem [16], cannot be symplectic. This is because a symplectic integrator cannot conserve energy exactly unless it produces the exact solution modulo time reparametrization. The fact that EEC algorithms cannot be symplectic can be demonstrated directly as follow: the basic evolution equation (29) can be derived from a Poisson bracket formulation [9] with Hamiltonian

$$H = \frac{1}{2m}\mathbf{p}^2, \tag{51}$$

but with a modified Poisson structure [17–19]

$$\{f,g\}_B = \frac{\partial f}{\partial \mathbf{q}} \cdot \frac{\partial g}{\partial \mathbf{p}} - \frac{\partial f}{\partial \mathbf{p}} \cdot \frac{\partial g}{\partial \mathbf{q}} - e\mathbf{B} \cdot \frac{\partial f}{\partial \mathbf{p}} \times \frac{\partial g}{\partial \mathbf{p}}. \tag{52}$$

It then follows that

$$\frac{dW}{dt} = \{W,H\}_B = \left[\mathbf{v} \cdot \frac{\partial}{\partial \mathbf{r}} + \omega(\hat{\mathbf{B}} \times \mathbf{v}) \cdot \frac{\partial}{\partial \mathbf{v}} \right] W, \tag{53}$$

where we have defined $\mathbf{r}=\mathbf{q}$ and $\mathbf{v}=\mathbf{p}/m$. This modified Poisson structure now implies that

$$\{q_i,q_j\} = 0, \quad \{q_i,p_j\} = \delta_{i,j} \tag{54}$$

and that

$$\{p_i,p_j\} = -e\,\delta_{ijk} B_k. \tag{55}$$

Since the fundamental set of Poisson brackets, Eq. (55), is noncanonical, the resulting algorithms cannot be canonical—i.e., symplectic.

IV. COMPARING SYMPLECTIC AND EXACT ENERGY-CONSERVING INTEGRATORS

We will first compare these two types of algorithms for a constant magnetic field in two dimensions (2D):

$$\hat{\mathbf{B}} = \hat{\mathbf{z}} \quad \text{with} \quad \omega = 1. \tag{56}$$

For a symplectic algorithm as described in Sec. II, choose $A_x=0$ and $A_y=(m/e)x$ so that $f_x=my$ and $f_y=mx$. Corre-

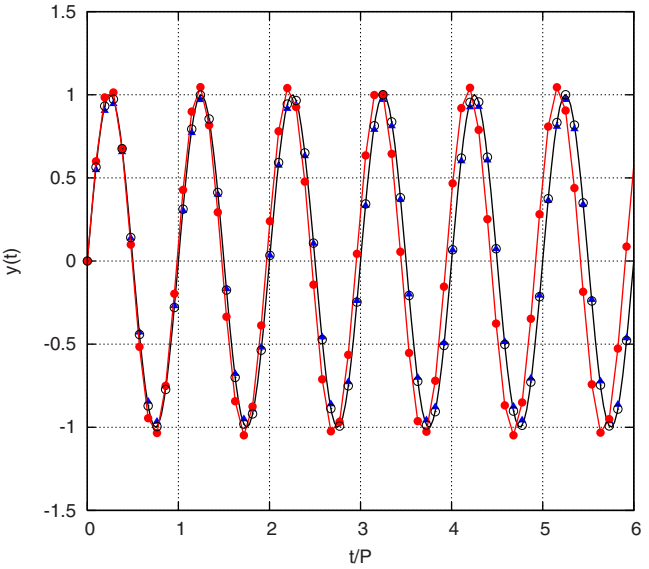

FIG. 1. (Color online) The y component of a 2D unit circle trajectory in a uniform magnetic field. The solid (black) line is the exact trajectory. Solid circles (red): symplectic algorithm S2b. Solid triangles (blue): exact energy conserving algorithm 2b. Open circle (black): exact algorithm $2b'$ of Appendix A. A large step size of $\varepsilon=0.6$ is used so that the phase error in S2b can be seen quickly. The period P is just 2π.

sponding to algorithm 2b would be the following symplectic algorithm S2b:

$$\mathcal{S}_{2b}(\varepsilon) = e^{(1/2)\varepsilon H_x} e^{\varepsilon H_y} e^{(1/2)\varepsilon H_x}. \tag{57}$$

Since $A_x=0$, only $e^{\varepsilon H_y}$ needs to be replaced by (14). [When implementing (14), because the factorization is not left-right symmetric, the resulting algorithm only works as expected when operators are applied from left to right, rather than right to left.] The initial condition $\mathbf{r}_0=(1,0)$, $\mathbf{v}_0=(0,1)$ produces a unit circle trajectory. In this case, the symplectic integrator is much simpler with no trigonometric function evaluations. However, even at this basic level, the difference between these two types of algorithm is huge. First, the EEC algorithm 2b is stable at all ε. (We define stability here as having a bounded trajectory no matter how long algorithm is run. The trajectory maybe highly inaccurate, but remains bounded.) The symplectic algorithm S2b is stable only for $\varepsilon \leq 2/\omega(=2)$, which is the well known stability criterion for a second-order symplectic integrator when solving the harmonic oscillator. The stability of EEC integrators is undoubtedly due to those trigonometric functions in (35), which are bounded function of the step size. Second, the EEC algorithm 2b has no phase error. Figure 1 compares their output for $y(t)$ at $\varepsilon=0.6$. Algorithm S2b's trajectory is slowly drifting out of phase with the exact solution. This is the well-known phase error of symplectic integrators when solving periodic motions [8,24,25]. This phase error increases linearly with time no matter how small the initial time step is. By contrast, EEC algorithm 2b showed no such error and is never far off from the exact position. (This is because its velocity is updated exactly.) This absence of (or much reduced) phase errors suggests that EEC algorithms are preferable to symplectic integrators in solving long-time periodic motion in a magnetic field, such as in an accelerator.

For comparing algorithms on a nonuniform magnetic field, we now take

$$\hat{\mathbf{B}} = \hat{\mathbf{z}} \quad \text{and} \quad \omega(x) = \frac{1}{x^2}, \tag{58}$$

and again only consider the nontrivial planar motion perpendicular to the field with $\mathbf{r}=\mathbf{r}_\perp=(x,y)$ and $\mathbf{v}=\mathbf{v}_\perp=(v_x,v_y)$. This choice was made with great care. We wanted a field configuration that produces typical charged-particle trajectories, is analytical solvable, has easy control over field strength variations, and most importantly, has another integral of motion besides the energy so that we can compare different ECC algorithms.

The trajectories in the field (58) can be solved with elementary methods [21]; we will just state the results. The initial condition can be taken to be $\mathbf{v}_0=(0,v_0)$ and $\mathbf{r}_0=(1,0)$ with one free parameter v_0. The x motion is periodic between

$$x_{\min} = \frac{1}{1+2v_0} \quad \text{and} \quad x_{\max} = 1, \tag{59}$$

with period

$$P = \frac{2\pi(1+v_0)}{(1+2v_0)^{3/2}}. \tag{60}$$

Associated with this period is a constant average angular velocity $\bar{\Omega}=2\pi/P$, but the actual angular velocity is not constant. By increasing v_0, one can force $x_{\min}$ closer to zero and subject the trajectory to greater magnetic field variations. The motion in the y direction is a constant drift, with *exact* drift velocity

$$v_d = \frac{v_0^2}{1+v_0}. \tag{61}$$

If this constant drift is removed via

$$y'(t) = y(t) - v_d t, \tag{62}$$

then $y'(t)$ is also periodic with

$$y'_{\min} = -\frac{v_0}{(1+v_0)\sqrt{1+2v_0}} \quad \text{and} \quad y'_{\max} = -y'_{\min}. \tag{63}$$

Thus $(x(t),y'(t))$ forms a closed ellipse that is useful for gauging the accuracy of any magnetic field integrator.

To produce the magnetic field (58), we choose $A_x=0$ and $A_y=-m/(ex)$, so that $f_x=my/x^2$ and $f_y=-m/x$. Since y is ignorable, the canonical velocity

$$\frac{p_y}{m} = v_y + \frac{1}{x} \tag{64}$$

is an integral of motion. This is exactly conserved by symplectic algorithms, but not by EEC algorithms. Thus the error in conserving p_y/m can be used to compare different EEC algorithms.

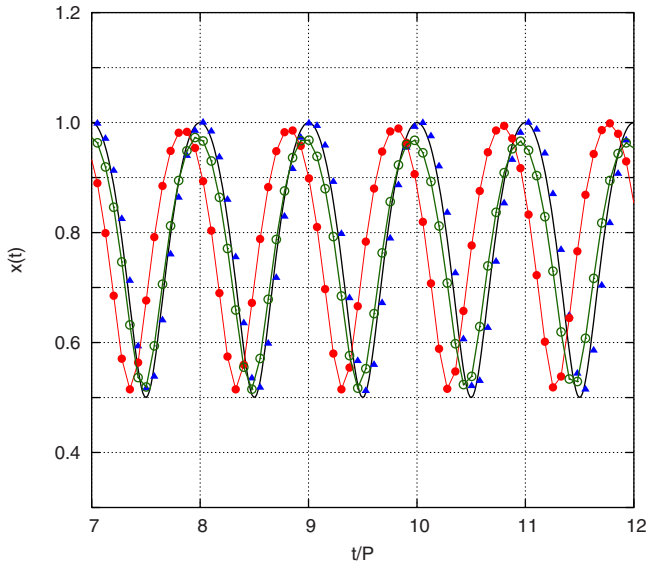

FIG. 2. (Color online) The x component of a 2D trajectory in a $1/x^2$ magnetic field. The solid (black) line is the "exact" trajectory computed by McLachlan's fourth-order algorithm at $\varepsilon=0.05$. Solid circles (red): symplectic algorithm S2b. Solid triangles (blue): exact energy-conserving algorithm 2b. Open circle (dark green): fourth-order Runge-Kutta. The step size used by these algorithms is $\varepsilon=0.2$.

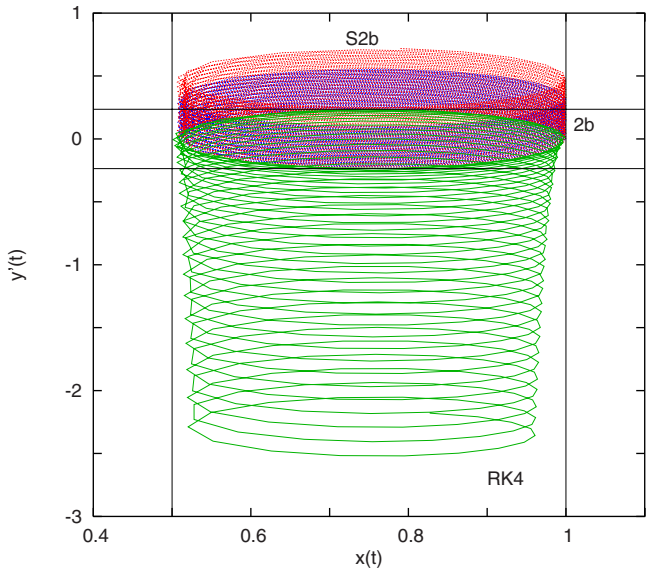

FIG. 3. (Color online) Reduced trajectories in which the exact vertical drift motion is removed. An exact trajectory would form a closed ellipse within the boxed rectangle. At $\varepsilon=0.2$, exact energy-conserving algorithm 2b has a smaller residual drift than symplectic algorithm S2b. RK4 denotes the fourth-order Runge-Kutta algorithm.

In Fig. 2, the periodic $x(t)$ for $v_0=1/2$ is computed at $\varepsilon=0.2$ using algorithms 2b and S2b and the standard fourth-order Runge-Kutta algorithm (RK4). In order to show the drifting phase error more clearly, we plotted $x(t)$ from period 7 to 12. While the phase error in S2b is glaring, 2b is also showing a very slight drift. However, one has to go all the way out to $t=60P$ to find 2b having the same phase drift as S2b at $t=6P$. The phase error in RK4 is also smaller than that of S2b, but its trajectory does not return to the starting value of $x_0=1$. Its solution deteriorates qualitatively with time. This is shown clearly in Fig. 3, where the reduced trajectories are shown for 35 periods. By comparison, both 2b and S2b remain qualitatively correct despite their inaccurate drift velocity. This is a hallmark usually associated with symplectic integrators. (The trajectory simply corresponds to a nearby Hamiltonian having a different drift velocity.) The EEC algorithm 2b shares this characteristic, but with a smaller drift velocity error.

Once a second-order splitting algorithm is known, the triplet construction [2,3] can be applied to yield the fourth-order Forest-Ruth (FR) integrator [1]

$$\mathcal{T}_{FR}(\varepsilon)=\mathcal{T}_2(a_1\varepsilon)\mathcal{T}_2(a_0\varepsilon)\mathcal{T}_2(a_1\varepsilon), \tag{65}$$

with

$$a_1=\frac{1}{2-2^{1/3}}\approx 1.35, \quad a_0=-\frac{2^{1/3}}{2-2^{1/3}}\approx -1.70 \tag{66}$$

and where $\mathcal{T}_2$ can be any second-order integrator such 2a or 2b. It is well known that the resulting FR integrator, which usually requires three field evaluations, has rather large errors. A far better choice is the class of integrators of the form

$$\mathcal{T}_M=\ldots\exp(\varepsilon t_0 T)\exp(\varepsilon v_1 V)\exp(\varepsilon t_1 T)\exp(\varepsilon v_2 V)\exp(\varepsilon t_2 T) \tag{67}$$

previously considered by McLachlan [22]. Since the algorithm is left-right symmetric, only operators from the center to the right are indicated. For a fourth-order integrator, the order condition requires [23] that

$$v_1=\frac{1}{2}-v_2, \quad t_2=\frac{1}{6}-4t_1v_1^2, \quad t_0=1-2(t_1+t_2), \tag{68}$$

$$w=\sqrt{3-12t_1+9t_1^2}, \quad v_2=\frac{1}{4}\left(1\mp\sqrt{\frac{9t_1-4\pm 2w}{3t_1}}\right), \tag{69}$$

with $t_1<0$ being a free parameter. There are four solution branches for v_2. The choice of

$$t_1=\frac{121}{3924}(12-\sqrt{471})\approx -0.299,$$

with

$$v_2=\frac{1}{4}\left(1+\sqrt{\frac{9t_1-4+2w}{3t_1}}\right), \tag{70}$$

reproduces McLachlan's [22] recommended algorithm (M). However, it is more advantageous to vary t_1 to optimize the algorithm for specific applications.

In Fig. 4, we repeated the reduced trajectory calculation of Fig. 3 using fourth-order algorithms. The triplet construction (65) can be applied to both 2b and S2b. At $\varepsilon=0.2$, these two fourth-order algorithms, denoted as FR(2b) and FR(S2b), are not better than their respective second-order

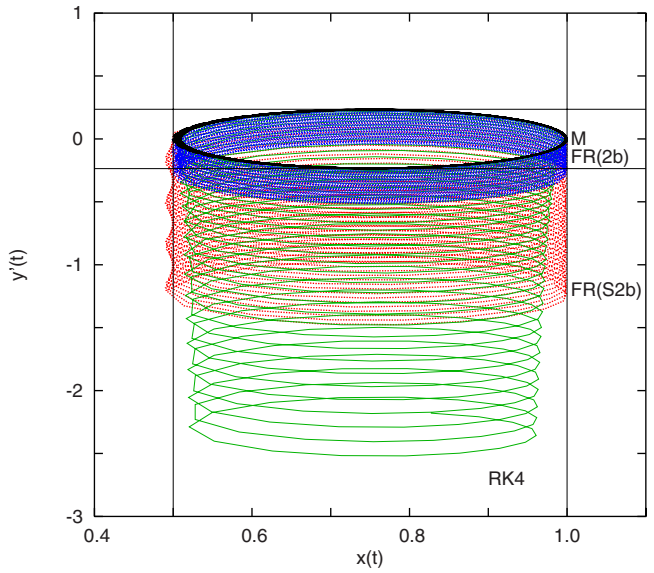

FIG. 4. (Color online) Reduced trajectories of fourth-order algorithms. FR(2b) is the Forest-Ruth integrator obtained by concatenating three 2b algorithms. FR(S2b) uses three symplectic S2b algorithms. The black thick line is the exact energy-conserving McLachlan algorithm M.

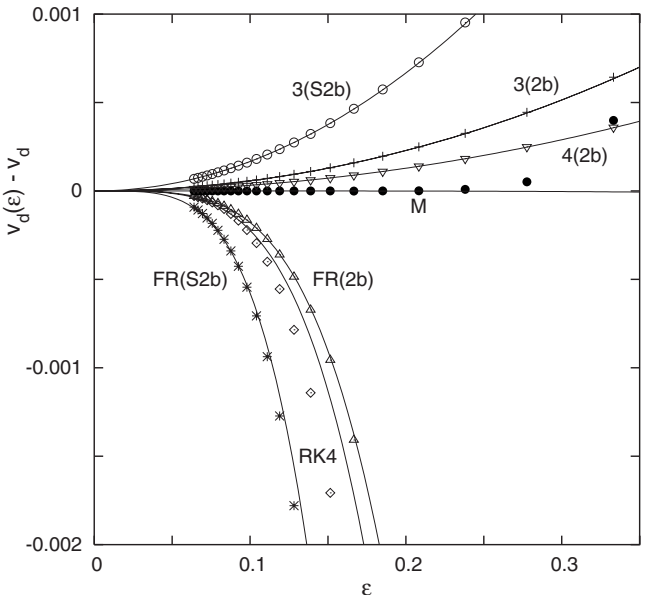

FIG. 5. The drift velocity error for various algorithms as a function of the step size ε. Lines are second- or fourth-order fits verifying the order of the algorithm. 3(2b) and 3(S2b) label results obtained by running second-order algorithms 2b and S2b three times at $\varepsilon/3$. 4(2b) labels results obtained by running algorithm 2b four times at $\varepsilon/4$.

algorithms. [In the case of FR(S2b), its drift velocity error is greater than that of S2b.] This suggests that the fourth-order convergence range of these two algorithms must be much smaller than $\varepsilon=0.2$. By comparison, McLachlan's algorithm is much better. To clarify this issue, we compute $v_d(\varepsilon)$ as a function of ε for each algorithm by dividing $y(t)$ after ten periods by $t=10P$. The results are shown in Fig. 5. As a control, we also plotted results obtained by updating the second-order algorithms 2b and S2b three times at time step $\varepsilon/3$ and 2b four times at $\varepsilon/4$. These are denoted as 3(2b), 3(S2b), and 4(2b), respectively. They are to be compared with FR(2b) and FR(S2b), which require three field evaluations, and RK4 and M, which require four field evaluations per update. Within the range of ε considered, the three fourth-order algorithms FR(2b), FR(S2b), and RK4 have greater error than the second-order integrator 2b using the same number of field-evaluations. Among fourth-order algorithms, FR(2b) is better than FR(S2b) and RK4. It is surprising, however, that the symplectic algorithm FR(S2b) has greater errors than RK4.

By comparison, McLachlan's algorithm (M) is far superior. Its error is also negative, but three orders of magnitude smaller than that of FR(2b). By fine-tuning $t_1=-0.277$, one can force this fourth-order error to vanish. However, since the error is already very small, this fine-tuning is indistinguishable from algorithm M's results on the scale of Fig. 5.

Since EEC algorithms cannot be symplectic, they cannot conserve the canonical velocity (64). This allows us to gauge different ECC algorithms by comparing their conservation of p_y/m. This is shown in Fig. 6. The error spikes at mid-period when $x(t)=x_{\min}$, where the magnetic field is the strongest. The behaviors of ECC and non-ECC integrators (such as RK4) here are exactly the same as symplectic and nonsymplectic integrators in conserving the energy. ECC algorithms conserve the canonical velocity periodically, bounded in time, whereas the error in non-ECC integrators grows linearly without bound. Despite RK4's much smaller initial fourth-order error, it soon exceeded that of FR(2b)'s. Algorithm M's error here is ≈50 times smaller than that of FR(2b).

Forward integrators with only positive splitting coefficients $\{t_i, v_i\}$ can be more efficient in solving classical dy-

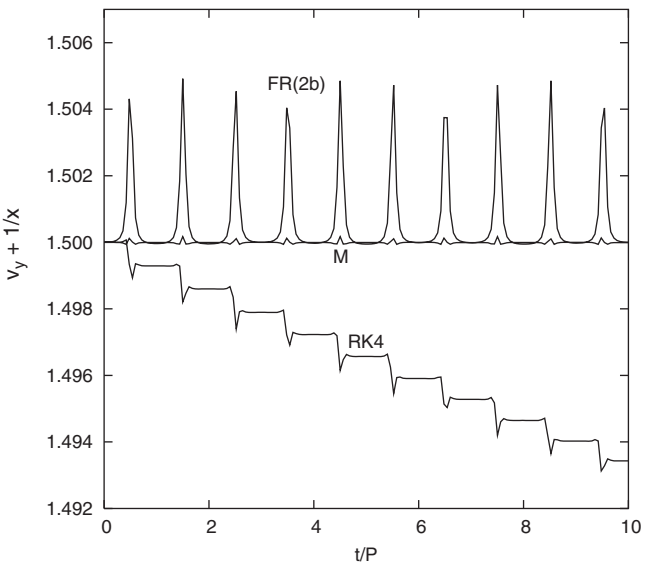

FIG. 6. The errors in the canonical velocity p_y/m as a function of time for fourth-order algorithms at $v_0=1/2$ and $\varepsilon=0.2$. Non-energy-conserving algorithms (such as RK4) are characterized by linearly growing errors. The error spikes at mid-period when $x(t)=x_{\min}$.

namics problems [8,14,23]. However, in order to devise a forward algorithm beyond second order, the exponential of either commutator $[T,[T,V]]$ or $[V,[T,V]]$ must be known exactly. Unfortunately, for a general magnetic field, the exponential of either commutators is more complicated than the original problem one is seeking to solve.

V. EXPONENTIAL-SPLITTING ALGORITHMS FOR ELECTRIC AND MAGNETIC FIELDS

If there is an additional force $\mathbf{F}(\mathbf{r})=q\mathbf{E}(\mathbf{r})$ so that

$$\frac{d\mathbf{v}}{dt}=\omega\hat{\mathbf{B}}\times\mathbf{v}+\mathbf{a}(\mathbf{r}), \tag{71}$$

where $\mathbf{a}(\mathbf{r})=\mathbf{F}(\mathbf{r})/m$, then V is modified to

$$V_{BF}=(\omega\hat{\mathbf{B}}\times\mathbf{v}+\mathbf{a})\cdot\frac{\partial}{\partial\mathbf{v}}. \tag{72}$$

One must now factorize the evolution operator $e^{\varepsilon(T+V_{BF})}$. This turns out to be just as easy since (71) can be solved *exactly* for arbitrary time-independent $\mathbf{B}(\mathbf{r})$ and $\mathbf{F}(\mathbf{r})$ fields,

$$\begin{aligned}\mathbf{v}_{BF}(\mathbf{r},\mathbf{v},\varepsilon)&=e^{\varepsilon V_{BF}}\mathbf{v}\\&=\mathbf{v}+(\theta\hat{\mathbf{B}}\times\mathbf{v}+\varepsilon\mathbf{a})+\frac{1}{2}\theta\hat{\mathbf{B}}\times(\theta\hat{\mathbf{B}}\times\mathbf{v}+\varepsilon\mathbf{a})\\&\quad+\frac{1}{3!}\theta\hat{\mathbf{B}}\times[\theta\hat{\mathbf{B}}\times(\theta\hat{\mathbf{B}}\times\mathbf{v}+\varepsilon\mathbf{a})]+\cdots\\&=\mathbf{v}+\theta(\hat{\mathbf{B}}\times\mathbf{v})+\frac{1}{2}\theta^2\hat{\mathbf{B}}\times(\hat{\mathbf{B}}\times\mathbf{v})\\&\quad+\frac{1}{3!}\theta^3\hat{\mathbf{B}}\times[\hat{\mathbf{B}}\times(\hat{\mathbf{B}}\times\mathbf{v})]+\cdots+\varepsilon\mathbf{a}\\&\quad+\varepsilon\frac{1}{2}\theta(\hat{\mathbf{B}}\times\mathbf{a})+\varepsilon\frac{1}{3!}\theta^2\hat{\mathbf{B}}\times(\hat{\mathbf{B}}\times\mathbf{a})+\cdots\\&=\mathbf{v}_B(\mathbf{r},\mathbf{v},\varepsilon)+\mathbf{v}_F(\mathbf{r},\mathbf{v},\varepsilon),\end{aligned} \tag{73}$$

where $\mathbf{v}_B(\mathbf{r},\mathbf{v},\varepsilon)$ is due to the magnetic field as before and $\mathbf{v}_F(\mathbf{r},\mathbf{v},\varepsilon)$ is due to the mixing of $\mathbf{a}(\mathbf{r})$ with $\mathbf{B}(\mathbf{r})$,

$$\begin{aligned}\mathbf{v}_F(\mathbf{r},\mathbf{v},\varepsilon)&\equiv\varepsilon\mathbf{a}+\frac{\varepsilon}{\theta}(1-\cos\theta)\hat{\mathbf{B}}\times\mathbf{a}\\&\quad+\varepsilon\left(1-\frac{\sin\theta}{\theta}\right)\hat{\mathbf{B}}\times(\hat{\mathbf{B}}\times\mathbf{a})\end{aligned} \tag{74}$$

$$=\varepsilon\mathbf{a}_{\parallel}+\frac{a_{\perp}}{\omega}[(1-\cos\theta)(\hat{\mathbf{B}}\times\hat{\mathbf{a}}_{\perp})+\sin\theta\hat{\mathbf{a}}_{\perp}]. \tag{75}$$

Here we again decompose $\mathbf{a}$ into components parallel and perpendicular to the local magnetic field $\mathbf{B}(\mathbf{r})$:

$$\mathbf{a}=\mathbf{a}_{\parallel}+\mathbf{a}_{\perp}. \tag{76}$$

The result (75) makes it clear how the magnetic field $\mathbf{B}(\mathbf{r})$ intertwines with the force field $\mathbf{a}(\mathbf{r})$ and causes $\mathbf{v}_{\perp}$ to gyrate in the plane perpendicular to the magnetic field with radius $a_{\perp}/\omega$. Note that $\mathbf{v}_F$ is identical in structure to $\mathbf{r}_B$. By comparing $\mathbf{v}_B(\mathbf{r},\mathbf{v},\varepsilon)$ and $\mathbf{v}_F(\mathbf{r},\mathbf{v},\varepsilon)$ we see that if $\hat{\mathbf{v}}_{\perp}=\hat{\mathbf{B}}\times\hat{\mathbf{a}}_{\perp}$, then automatically $\hat{\mathbf{B}}\times\hat{\mathbf{v}}_{\perp}=-\hat{\mathbf{a}}_{\perp}$, and a charged particle with a local velocity

$$\mathbf{v}_{\perp}=\frac{a_{\perp}}{w}\hat{\mathbf{v}}_{\perp} \tag{77}$$

will not be deflected by the combined force fields. This is just the well-known $\mathbf{E}\times\mathbf{B}$ velocity-selector effect.

Since $e^{\varepsilon V_{BF}}$ is known exactly, exponential-splitting integrators of any order can again be derived by factorization as before. For example, we have two standard second-order algorithms

$$\mathcal{T}_{2a}=e^{(1/2)\varepsilon V_{BF}}e^{\varepsilon T}e^{(1/2)\varepsilon V_{BF}}, \tag{78}$$

$$\mathcal{T}_{2b}=e^{(1/2)\varepsilon T}e^{\varepsilon V_{BF}}e^{(1/2)\varepsilon T}, \tag{79}$$

and fourth-order algorithms follow as before. Algorithm 2a is again the generalization of the velocity-Verlet integrator, which has been previously derived by Spreiter and Walter [26], but without recognizing its exponential-splitting character. A leapfrog-type algorithm, corresponding to the first-order splitting

$$\mathcal{T}=e^{\varepsilon T}e^{\varepsilon V_{BF}}, \tag{80}$$

but with a further second-order splitting $(V_F=\mathbf{a}\cdot\frac{\partial}{\partial\mathbf{v}})$

$$e^{\varepsilon V_{BF}}=e^{(1/2)\varepsilon V_F}e^{\varepsilon V}e^{(1/2)\varepsilon V_F}, \tag{81}$$

has been widely used in plasma physics simulations [27]. Since the splitting (81) is only second order, this approximation for $e^{\varepsilon V_{BF}}$ cannot be used in a general higher-order algorithm.

For a nonuniform electric and magnetic field, these exponential-splitting algorithms are neither symplectic nor exactly energy conserving. However, as we will see in the next section, their numerical characteristics are identical to those of symplectic integrators. When both the electric and magnetic fields are constant, one can again derive exact algorithms. This is done in Appendix B.

Again, time-dependent fields can be solved by applying Suzuki's rule.

VI. COMPARING INTEGRATORS FOR NONUNIFORM MAGNETIC AND FORCE FIELDS

To compare various algorithms, we test them against a nontrivial periodic orbit in a 2D harmonic force field $\mathbf{a}=-\mathbf{r}$ and a 2D axial-symmetric magnetic field:

$$\hat{\mathbf{B}}=\hat{\mathbf{z}}\quad\text{with}\quad\omega(\mathbf{r})=\frac{1}{r}, \tag{82}$$

where $r=\sqrt{x^2+y^2}$. The noncanonical Hamiltonian to be used with the modified Poisson structure (52) is then

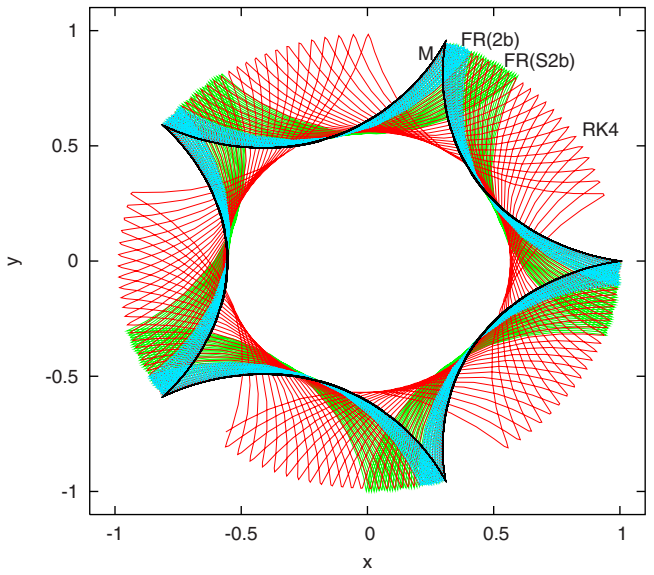

FIG. 7. (Color online) A closed orbit computed of fourth-order algorithms in a harmonic force field and a $1/r$ magnetic field at $\varepsilon=0.2$. RK4's precession error grows with time. Algorithm M's precession error (solid, black line) is 50 times smaller than that of FR(2b) while symplectic algorithm FR(S2b)'s error is more than twice that of FR(2b).

$$H=\frac{1}{2}(p_x^2+p_y^2)+\frac{1}{2}(x^2+y^2). \tag{83}$$

This combination of force fields has many unusual closed orbits with cusps. The initial values $\mathbf{r}=(1,0)$ and $\mathbf{v}=(0,-0.01175)$ produce a five-pointed star orbit. To implement symplectic algorithms, we use the vector potential $A_x=0$ and $A_y=(m/e)\ln(x+r)$ with $f_x=m\ln(y+r)$ and $f_y=m\ln(x+r)$. The use of the vector potential here introduces more complicated functions f_x and f_y than those needed to describe the magnetic field. In this case, there are no ignorable coordinates and no other obvious integral except the Hamiltonian. Figure 7 shows the trajectories produced by four fourth-order algorithms at $\varepsilon=0.2$ for 30 orbital periods. Since the problem is axially symmetric, the easiest way for an orbit to go wrong is to rotate, resulting in a precession error [28]. Symplectic algorithms are not immune from this error (a form of the phase error). While their energy errors are bounded and periodic, this precession error can again grow linearly with time. The exponential-splitting algorithms seem to have smaller precession errors than the symplectic integrator FR(S2b). To quantify this, we compute the precession angle after each period as a function of the step size in Fig. 8. Despite a completely different problem, the performance of various fourth-order algorithms remains strikingly similar to the drift velocity calculation in Fig. 5. Here, the symplectic algorithm S2b is better than 2b, yet FR(S2b) is still worse than FR(2b) and RK4. One advantage of a higher-order algorithm is that one can use a much larger step size to achieve the same accuracy of a lower-order algorithm. While algorithm M achieved this goal spectacularly, algorithms FR(S2b), FR(2b), and RK4 are not competitive with second-order algorithms until the step size is very small.

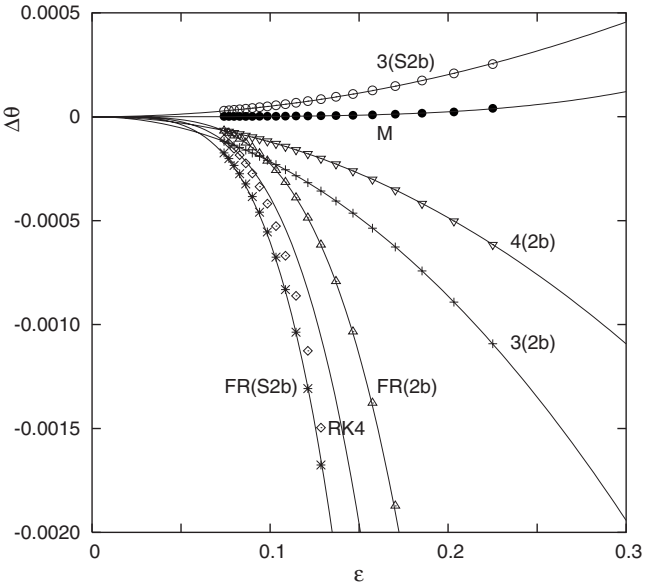

FIG. 8. The error precession angle after each period as produced by various algorithms in solving the star orbit of Fig. 7. The solid lines are second- or fourth-order order fits made to verify the order of convergence. All are very well fitted except RK4, suggesting that its convergence range is at $\varepsilon \lesssim 0.1$.

Figure 9 shows the energy error coefficients of the same four fourth-order algorithms. This is extracted by dividing the energy error by ε^4 at smaller and smaller ε until the result no longer depends on ε. This convergence is achieved for all algorithms except RK4 at $\varepsilon \lesssim 0.1$. For RK4, its energy error is growing linearly with time, but the slope continues to decrease with ε. Figure 9 is computed at $\varepsilon=P/300\approx 0.04$. The maximum energy error height of FR(S2b) is 30 times that of FR(2b), while the maximum energy error height of M is only

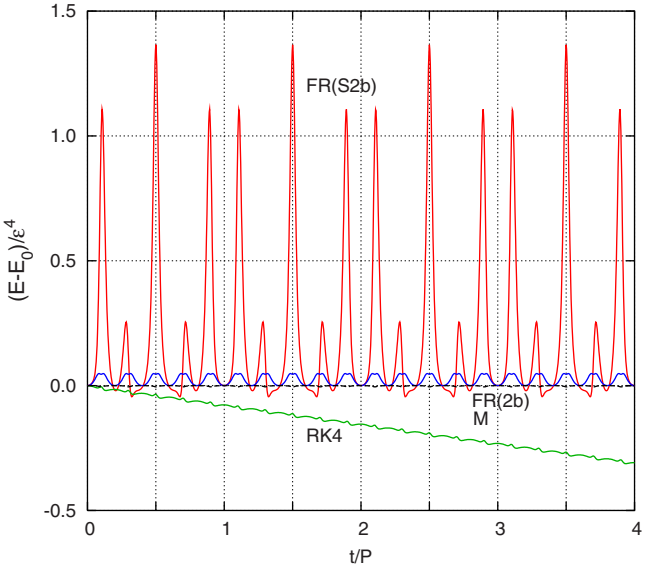

FIG. 9. (Color online) The energy error coefficient of fourth-order algorithms in solving the star orbit of Fig. 7. Exponential-splitting algorithms FR(2b) and M have periodic energy errors, just like the symplectic integrator FR(S2b), only much smaller. M is the horizontal dashed black line barely distinguishable from zero.

a tenth of FR(2b). The energy error of all algorithms, except RK4, returns to zero periodically. This is usually a distinguishing feature of symplectic algorithms. Figure 9 shows that this is a common characteristic of all exponential-splitting algorithms. When in an electric and magnetic field, they are neither fully symplectic nor exactly energy conserving, yet they conserve energy periodically better than the symplectic integrator FR(S2b).

VII. CONCLUSIONS

For a separable Hamiltonian, exponential splitting results in algorithms that are symplectic. For solving trajectories in a magnetic field, exponential splitting of a noncanonical evolution operator results in algorithms that are exactly energy conserving. For a combined electric and magnetic field, these noncanonical splitting algorithms are neither fully symplectic nor exactly energy conserving, yet they behave identically as symplectic and EEC algorithms in having qualitatively correct trajectories and bounded periodic energy errors. This suggests that exponential splitting is a general method of producing efficient algorithms and symplectic and EEC algorithms are just special cases depending on the form of the equations of motion.

The key advance which make exponential splitting possible for magnetic field problems is the recognition that the Lorentz force law can be exactly solved by use of the rotation operator of quantum mechanics. Since the Lorentz force law is isomorphic to rigid-body dynamics [7] and spin dynamics [29], the exponential-splitting algorithms developed here can also be profitably applied to these important areas of computational physics.

For computing magnetic field trajectories, this work demonstrated that exponential-splitting algorithms are simpler to derive, easier to implement (no vector potential needed), intrinsically more stable, and have far less phase error than symplectic integrators. These algorithms should be further tested on more realistic systems of physical interest.

As a by-product of our comparative study, we have shown again that Forest-Ruth-type fourth-order integrators based on the triplet construction have rather large errors. They are far outperformed by McLachlan-type algorithms, which must be derived individually.

APPENDIX A: EXACT ALGORITHMS FOR A UNIFORM MAGNETIC FIELD

For a constant magnetic field, since $TV^n\mathbf{v}=0$, Eq. (32) can be solved directly,

$$\mathbf{v}(\varepsilon) = e^{\varepsilon(T+V)}\mathbf{v} = e^{\varepsilon V}\mathbf{v} = \mathbf{v}_B(\mathbf{r},\mathbf{v},\varepsilon) \tag{A1}$$

and

$$\begin{aligned}\mathbf{r}(\varepsilon) &= e^{\varepsilon(T+V)}\mathbf{r}\\ &= \left(1+\varepsilon(T+V)+\frac{1}{2}\varepsilon^2(T+V)^2+\cdots\right)\mathbf{r}\\ &= \mathbf{r}+\varepsilon\mathbf{v}+\varepsilon\left(\frac{1}{2!}\theta(\hat{\mathbf{B}}\times\mathbf{v})+\frac{\theta^2}{3!}\hat{\mathbf{B}}\times(\hat{\mathbf{B}}\times\mathbf{v})+\cdots\right)\\ &= \mathbf{r}_B(\mathbf{r},\mathbf{v},\varepsilon),\end{aligned} \tag{A2}$$

where

$$\mathbf{r}_B(\mathbf{r},\mathbf{v},\varepsilon) \equiv \mathbf{r}+\varepsilon\mathbf{v}+\frac{\varepsilon}{\theta}(1-\cos\theta)(\hat{\mathbf{B}}\times\mathbf{v}) + \varepsilon\left(1-\frac{\sin\theta}{\theta}\right)\hat{\mathbf{B}}\times(\hat{\mathbf{B}}\times\mathbf{v}) \tag{A3}$$

$$= \mathbf{r}+\varepsilon\mathbf{v}_{\parallel}+\frac{v_{\perp}}{\omega}[(1-\cos\theta)(\hat{\mathbf{B}}\times\hat{\mathbf{v}}_{\perp})+\sin\theta\hat{\mathbf{v}}_{\perp}] \tag{A4}$$

and $v_{\perp}/\omega$ is the cyclotron radius.

To illustrate the kind of analysis that can be done with this operator approach, we will now show that this exact solution can be derived as an exponential-splitting algorithm. For a constant magnetic field, the only nonvanishing commutators are of the form $[V^nT]$, where the set of condensed brackets means $[V^3T]=[V,[V,[V,T]]]$, etc. In particular,

$$[VVT] = \omega^2\hat{\mathbf{B}}\times(\hat{\mathbf{B}}\times\mathbf{v})\cdot\frac{\partial}{\partial\mathbf{r}}, \tag{A5}$$

and because of (38),

$$[V^2V^{2n}T] = -\omega^2[V^{2n}T]. \tag{A6}$$

Since the factorization scheme (44) is left-right symmetric, only error commutators even in V can appear on the RHS of (45). Moreover, Laskar and Robutel [20] have shown that all error coefficients of the commutators $[V^nT]$ on the RHS of (45) are known to all orders:

$$\begin{aligned}W &= V+\frac{\frac{1}{2}\varepsilon[V,\cdot]}{\sinh\left(\frac{1}{2}\varepsilon[V,\cdot]\right)}T\\ &= V+T-\frac{1}{24}\varepsilon^2[V^2T]\\ &\quad+\frac{7}{5760}\varepsilon^4[V^4T]+\cdots.\end{aligned} \tag{A7}$$

Because of (A6), we have, presently,

$$\begin{aligned}W &= V+T-\left(\frac{1}{24}\theta^2+\frac{7}{5760}\theta^4+\cdots\right)\frac{1}{\omega^2}[V^2T]\\ &= V+T+\left[1-\frac{(\theta/2)}{\sin(\theta/2)}\right]\frac{1}{\omega^2}[V^2T].\end{aligned} \tag{A8}$$

All the error terms above can now be eliminated by replacing $T\to\tilde{T}$, where

$$\tilde{T} = T+g(\theta)\frac{1}{\omega^2}[V^2T] = [\mathbf{v}+g(\theta)\hat{\mathbf{B}}\times(\hat{\mathbf{B}}\times\mathbf{v})]\cdot\frac{\partial}{\partial\mathbf{r}}, \tag{A9}$$

with

$$g(\theta) = 1 - \frac{\sin(\theta/2)}{(\theta/2)}. \tag{A10}$$

Thus one has an exact factorization

$$e^{\varepsilon(T+V)} = e^{(1/2)\varepsilon V} e^{\varepsilon \tilde{T}} e^{(1/2)\varepsilon V}. \tag{A11}$$

On can check that the resulting algorithm 2a′,

$$\mathbf{v}_1 = \mathbf{v}_B\left(\mathbf{r}, \mathbf{v}, \frac{1}{2}\varepsilon\right),$$

$$\mathbf{r}_1 = \mathbf{r} + \varepsilon[\mathbf{v}_1 + g(\theta)\hat{\mathbf{B}} \times (\hat{\mathbf{B}} \times \mathbf{v}_1)],$$

$$\mathbf{v}_2 = \mathbf{v}_B\left(\mathbf{r}_1, \mathbf{v}_1, \frac{1}{2}\varepsilon\right), \tag{A12}$$

gives the exact solution (A3). (For a constant magnetic field, $\mathbf{v}_B$ has no spatial dependence.)

Similarly, one can also factorize exactly in the form of

$$e^{\varepsilon(T+V)} = e^{(1/2)\varepsilon T^*} e^{\varepsilon V} e^{(1/2)\varepsilon T^*}, \tag{A13}$$

where now the error terms are

$$W = V + \frac{\frac{1}{2}\varepsilon[V,\cdot]}{\tanh\left(\frac{1}{2}\varepsilon[V,\cdot]\right)} T = V + T + \left[1 - \frac{(\theta/2)}{\tan(\theta/2)}\right]\frac{1}{\omega^2}[V^2 T] \tag{A14}$$

and can be eliminated by choosing

$$T^* = [\mathbf{v} + h(\theta)\hat{\mathbf{B}} \times (\hat{\mathbf{B}} \times \mathbf{v})] \cdot \frac{\partial}{\partial \mathbf{r}}, \tag{A15}$$

with

$$h(\theta) = 1 - \frac{\tan(\theta/2)}{(\theta/2)}. \tag{A16}$$

The resulting algorithm 2b′ is

$$\mathbf{r}_1 = \mathbf{r} + \frac{1}{2}\varepsilon[\mathbf{v} + h(\theta)\hat{\mathbf{B}} \times (\hat{\mathbf{B}} \times \mathbf{v})],$$

$$\mathbf{v}_1 = \mathbf{v}_B(\mathbf{r}_1, \mathbf{v}, \varepsilon),$$

$$\mathbf{r}_1 = \mathbf{r}_1 + \frac{1}{2}\varepsilon[\mathbf{v}_1 + h(\theta_1)\hat{\mathbf{B}}_1 \times (\hat{\mathbf{B}}_1 \times \mathbf{v}_1)]. \tag{A17}$$

We have generalized both algorithms 2a′ and 2b′ to the case where $\mathbf{B}$ is nonuniform, so that θ_1 and $\hat{\mathbf{B}}_1$ refer to the magnetic field evaluated at $\mathbf{r}_1$. However, when the magnetic field is nonuniform, the algorithmic steps in (A12) and (A17) no longer correspond to an exact evaluation of $e^{\varepsilon \tilde{T}}$ and $e^{\varepsilon T^*}$ and both algorithms cease to be truly exponential-splitting algorithms.

APPENDIX B: CONSTANT ELECTRIC AND MAGNETIC FIELD INTEGRATORS

If both $\mathbf{B}$ and $\mathbf{a}$ are constant, then the position vector can also be determined:

$$\begin{aligned}\mathbf{r}_{BF}(\mathbf{r},\mathbf{v},\varepsilon) &= e^{\varepsilon(T+V_{BF})}\mathbf{r} \\ &= \mathbf{r} + \varepsilon\mathbf{v} + \varepsilon\left(\frac{1}{2}(\theta\hat{\mathbf{B}} \times \mathbf{v} + \varepsilon\mathbf{a})\right. \\ &\quad \left. + \frac{1}{3!}\theta\hat{\mathbf{B}} \times (\theta\hat{\mathbf{B}} \times \mathbf{v} + \varepsilon\mathbf{a}) + \cdots\right) \\ &= \mathbf{r} + \varepsilon\mathbf{v} + \varepsilon\left(\frac{1}{2}\theta(\hat{\mathbf{B}} \times \mathbf{v}) + \frac{\theta^2}{3!}\hat{\mathbf{B}} \times (\hat{\mathbf{B}} \times \mathbf{v}) + \cdots\right) \\ &\quad + \varepsilon^2\left(\frac{1}{2}\mathbf{a} + \frac{1}{3!}\theta\hat{\mathbf{B}} \times \mathbf{a} + \frac{1}{4!}\theta^2\hat{\mathbf{B}} \times (\hat{\mathbf{B}} \times \mathbf{a}) + \cdots\right) \\ &= \mathbf{r}_B(\mathbf{r},\mathbf{v},\varepsilon) + \mathbf{r}_F(\mathbf{r},\mathbf{v},\varepsilon),\end{aligned} \tag{B1}$$

where

$$\begin{aligned}\mathbf{r}_F(\mathbf{r},\mathbf{v},\varepsilon) &= \frac{1}{2}\mathbf{a}\varepsilon^2 + \frac{\varepsilon^2}{\theta}\left(1 - \frac{\sin\theta}{\theta}\right)(\hat{\mathbf{B}} \times \mathbf{a}) \\ &\quad + \varepsilon^2\left(\frac{1}{2} - \frac{1-\cos\theta}{\theta^2}\right)\hat{\mathbf{B}} \times (\hat{\mathbf{B}} \times \mathbf{a}) \\ &= \frac{1}{2}\mathbf{a}_\parallel\varepsilon^2 + \frac{1}{\omega^2}[(\theta - \sin\theta)\hat{\mathbf{B}} \times \mathbf{a}_\perp + (1-\cos\theta)\mathbf{a}_\perp].\end{aligned} \tag{B2}$$

We can again modify (78) and (79) to be exact when both $\mathbf{B}$ and $\mathbf{a}$ are constant. With the addition of $\mathbf{a}$, the generalization of (A6) now reads

$$[V_{BF}^{2n} T] = (-1)^{n-1}\omega^{2n}\hat{\mathbf{B}} \times \left(\hat{\mathbf{B}} \times \mathbf{v} + \frac{1}{\omega}\mathbf{a}\right) \cdot \frac{\partial}{\partial \mathbf{r}}, \tag{B3}$$

yielding exact algorithms

$$\mathcal{T}_{2a'} = e^{(1/2)\varepsilon V_{BF}} e^{\varepsilon \tilde{T}_F} e^{(1/2)\varepsilon V_{BF}}, \tag{B4}$$

with

$$\tilde{T}_F = \left[\mathbf{v} + g(\theta)\hat{\mathbf{B}} \times \left(\hat{\mathbf{B}} \times \mathbf{v} + \frac{1}{\omega}\mathbf{a}\right)\right] \cdot \frac{\partial}{\partial \mathbf{r}} \tag{B5}$$

and

$$\mathcal{T}_{2b'} = e^{(1/2)\varepsilon T_F^*} e^{\varepsilon V_{BF}} e^{(1/2)\varepsilon T_F^*}, \tag{B6}$$

with

$$T_F^* = \left[\mathbf{v} + h(\theta)\hat{\mathbf{B}} \times \left(\hat{\mathbf{B}} \times \mathbf{v} + \frac{1}{\omega}\mathbf{a}\right)\right] \cdot \frac{\partial}{\partial \mathbf{r}}. \tag{B7}$$

Again, these algorithms, while of interest because they are exact for constant fields, are not truly exponential-splitting algorithms when integrating nonuniform fields.

[1] E. Forest and R. D. Ruth, Physica D **43**, 105 (1990).
[2] M. Creutz and A. Gocksch, Phys. Rev. Lett. **63**, 9 (1989).
[3] H. Yoshida, Phys. Lett. A **150**, 262 (1990).
[4] H. Yoshida, Celestial Mech. Dyn. Astron. **56**, 27 (1993).
[5] E. Hairer, C. Lubich, and G. Wanner, *Geometric Numerical Integration* (Springer-Verlag, Berlin, 2002).
[6] R. I. McLachlan and G. R. W. Quispel, Acta Numerica **11**, 241 (2002).
[7] B. Leimkuhler and S. Reich, *Simulating Hamiltonian Dynamics* (Cambridge University Press, Cambridge, England, 2004).
[8] S. R. Scuro and S. A. Chin, Phys. Rev. E **71**, 056703 (2005).
[9] A. J. Dragt and J. M. Finn, J. Math. Phys. **17**, 2215 (1976).
[10] Y. K. Wu, E. Forest, and D. S. Robin, Phys. Rev. E **68**, 046502 (2003).
[11] E. Merzbacher, *Quantum Mechanics*, 3rd ed. (Wiley, New York, 1998).
[12] M. Suzuki, Proc. Jpn. Acad., Ser. B: Phys. Biol. Sci. **69**, 161 (1993).
[13] S. A. Chin and C. R. Chen, J. Chem. Phys. **117**, 1409 (2002).
[14] S. A. Chin and C. R. Chen, Celestial Mech. Dyn. Astron. **91**, 301 (2005).
[15] S. A. Chin and P. Anisimov, J. Chem. Phys. **124**, 054106 (2006).
[16] Ge Zhong and J. E. Marsden, Phys. Lett. A **133**, 134 (1988).
[17] J. E. Marsden, *Lectures on Mechanics* (Cambridge University Press, Cambridge, England, 1992).
[18] M. Mantoiu and R. Purice, in *Mathematical Physics of Quantum Mechanics*, edited by J. Asch and A. Alain, Lecture Notes in Physics Vol. 690 (Springer, Heidelberg, 2006), p. 417.
[19] F. J. Vanhecke, C. Sigaud, and A. R. da Silva, Braz. J. Phys. **36**, 194 (2006).
[20] J. Laskar and P. Robutel, Celestial Mech. Dyn. Astron. **80**, 39 (2001).
[21] P. C. Clemmow and J. P. Dougherty, *Electrodynamics of Particles and Plasmas* (Addison-Wesley, Reading, MA, 1969).
[22] R. I. McLachlan, SIAM J. Sci. Comput. **16**, 151 (1995).
[23] S. A. Chin, Int. J. Comput. Math. **84**, 729 (2007).
[24] H. Kinoshita, H. Yoshida, and H. Nakai, Celestial Mech. **50**, 59 (1991).
[25] B. Gladman, M. Duncan, and J. Candy, Celestial Mech. **52**, 221 (1991).
[26] Q. Spreiter and M. Walter, J. Comput. Phys. **152**, 102 (1999).
[27] C. K. Birdsall and A. B. Landon, *Plasma Physics via Computer Simulation* (Adam Hilger, Bristol, 1991), pp. 13–15 and 58–63.
[28] S. A. Chin, Phys. Rev. E **75**, 036701 (2007).
[29] S. H. Tsai, M. Krech, and D. P. Landau, Braz. J. Phys. **34**, 384 (2004).